Direct-contact condensation from vapour- gas mixture in a spray ejector condenser for negative CO_2 power plant

Dariusz Mikielewicz[1*], Milad Amiri[1#], Jaroslaw Mikielewicz[2]

[1] *Gdańsk University of Technology, Faculty of Mechanical Engineering and Ship Technology, Poland*
[2] *Institute of Fluid Flow Machinery, Polish Academy of Sciences, Gdańsk, Poland*

**Corresponding Author, dariusz.mikielewicz@pg.edu.pl*
[#]Presenting Author, milad.amiri@pg.edu.pl

Abstract

Direct-contact condensation of vapour containing the inert gas on a spray of subcooled liquid exists in a number of technical applications. For example, it may be found in the nuclear industry (e.g. pressurized jet under normal operating conditions, in safety analyses) or in the chemical industry (e.g. mixing-type heat exchanger, degasser, sea water desalting). The problem is also essential to modelling and analysis of some fundamental phenomena of two phase flow, such as condensation in power engineering condenser of steam power plant as well as a new concept of negative CO_2 power plant, where separation of carbon dioxide from the mixture of steam and inert gas takes place in the spray ejector condenser (SEC) followed by the centrifugal separation in the cyclone. The phenomenon of direct-condensation heat transfer is primarily characterized by the appropriate transport of heat and mass through a moving vapour-liquid interface. Furthermore, using a spray ejector condenser (SEC) with separators can be considered as an alternative method to increase the efficiency of separation process. The present survey attempts to investigate the effect of different initial velocity of mixture and droplet on their temperature as well as the effect of diameter of throat on temperature of droplet and mixture.

For the ejector design, the study focuses on the ejector nozzle, pre-mixing chamber, the mixing section and the diffuser. Flow properties and ejector geometry are considered using the thermodynamic equations, conservation equations and other assumptions established based on literature. Comparisons with experimental data show a good consistency with experimental results. Results show that increasing the value of initial velocity of mixture of steam (Um0) not only results in increasing the temperature of droplet, but also leads to rise the temperature of mixture of steam at the length of throat. Moreover, the lowest value for temperature of droplet and mixture of steam is when the drop is moving in stagnant environment ($um(x) = 0$).

Keywords : spray ejector condenser, direct-contact condensation, analytical modelling, breakup

1. Introduction

Direct-contact condensation plays a pivotal role for both engineering and natural sciences that has been exploited in many fields [1-5]. Direct contact condensation (DCC) befalls when a gas/vapour stream comes into contact with a subcooled liquid, and is associated with high heat transfer coefficients because there are no partitions as in conventional heat exchange procedures [6]. Li et al. [7], Zhu et al. [8] and Jayachandran et al. [9-11] reported a typical application of direct contact condensers at cryogenic temperatures where the hot oxygen gas driving the turbine mixes with the subcooled liquid oxygen from the pump at the output of the booster turbopump of a cryogenic rocket engine operating in a staged combustion cycle. Li et al. [12] used the VOF approach in ANSYS Fluent® to investigate the vertical injection of steam jets into subcooled flowing water in a T-junction and found good agreement with experimental results.

In addition, the condensation of vapour on a spray of drops is a very complicated process. Drop size distribution, drop velocity, and condensation on droplets should be investigated in order to characterize it. A jet coming out of the nozzle dissipates and breaks up into various-sized drops. Condensation of vapour on the drops occurs when saturated vapour comes into contact with subcooled drops (their temperature is lower than the saturation temperature of the vapour at the given pressure) and the size of the drops is larger than the critical value. If the droplets size is smaller than critical size, droplets will evaporate.

Furthermore, the droplet breakup, depending on the relative velocity between the flow and droplet, as defined by the Weber number (the ratio of the aerodynamic force over the surface tension). Droplet breakup behaviours are characterized into bag, oscillation, multimode, catastrophic and shear breakup patterns as the Weber number increases. As a result, several experimental research has been conducted to investigate the drop evolution process, and numerous formulas and models to characterize the breakup behaviours have been developed. Li et al [13] used the established digital in-line holography technique to evaluate the secondary droplet size distribution after the breakup of a sub-millimetre droplet under high velocity cross flow circumstances on a horizontal shock tube. With three-dimensional modeling [14-16], a variety of breakup behaviours and flow field structures, such as wrinkles on the droplet surface, surface waves and vortex shedding phenomena, were visibly exhibited, considerably aiding researchers' understanding of the breakup phenomena. Shen et al [17, 18] experimentally studied the effect of droplet viscosity on the breakup behaviour of droplets which is more relevant for real detonation engines.

In this paper, an analytical methodology has been adopted, so that the purpose of study is not only investigation heat and mass transfer of droplets and mixture with and without condensation, but also the effect of different initial velocity of mixture and droplet on their temperature have been scrutinized. In addition, the effect of diameter of droplet and throat on temperature of droplet and mixture has been studied. Moreover, effect of breakup of droplet investigated and best estimate for diameter of droplets has been obtained.

2. Physical ejector model and its mathematical description

The theoretical analysis in the paper concerns the issue of direct-contact condensation of vapour with inert gas within ejector creating a subcooled water spray. The physical situation considered is shown in Fig. 1.

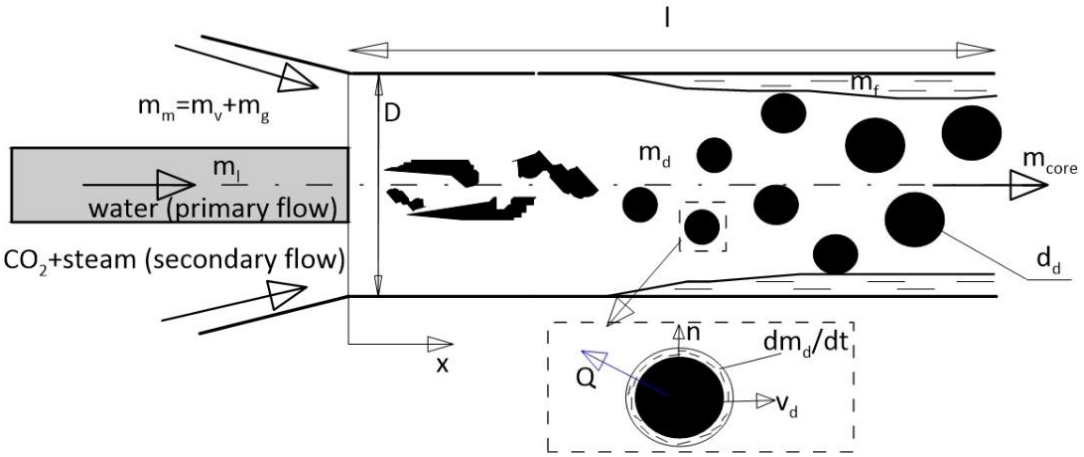

Fig. 1. Schematic of the nozzle

In order to maximize the device efficiency a proper ejector design and analysis is required. The ejector, being the critical component of the system, determines the overall performance and efficiency of the condensing steam from mixture of vapour-noncondensing gas system. Adiabatic irreversible flow model is used for the ejector analysis, wherein frictional losses through the ejector are considered. For the ejector design, the study focuses on the ejector nozzle, pre-mixing chamber, mixing section and the diffuser. Flow properties and ejector geometry are considered using the thermodynamic equations, conservation equations and other assumptions established based on literature.

2.1 Pre-mixing Chamber

The considered spray ejector condenser is basically a converging-diverging nozzle with the condensation section inside. Fig. 2 demonstrates the division of the ejector into elementary control volumes from the inlet up to the exit.

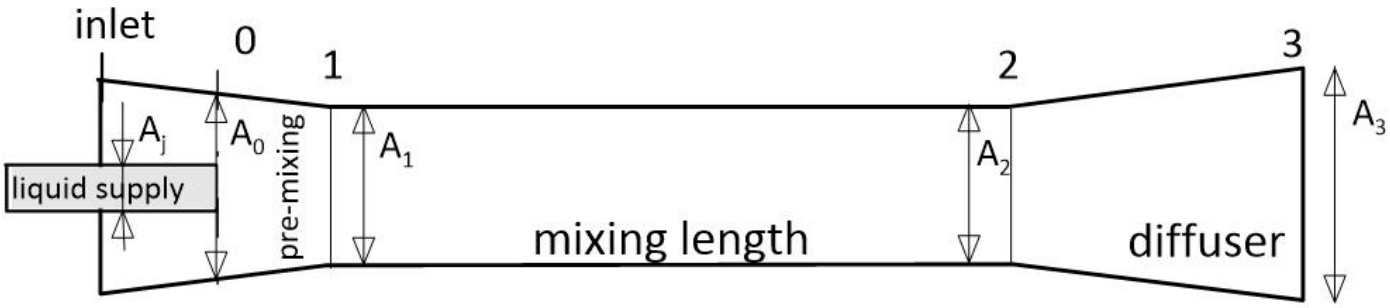

Fig. 2. General outlay of the ejector

It is assumed that the inlet properties of the fluids, which are supplied at a state denoted as "inlet" in Fig. 2, are all known. At that location the liquid jet has a subscript l (j) whereas the mixture of vapour and non-condensable is denoted as g.
In order to calculate, for a particular ejector design, the suction mass and the pressure at the beginning of the mixing zone, it is necessary to know the equation resulting from the flow in the inlet zone resulting from Bernoulli's equation for a real liquid:

$$p_{g,inlet} + \frac{1}{2} \cdot \rho_{g,0} u_{g,inlet}^2 = p_{g,0} + \frac{1}{2} \cdot \rho_{g,0} u_{g,0}^2 + \Delta p_{loss,1} \quad (1)$$

The pressure drop due to losses can be evaluated from the local losses:

$$\Delta p_{loss,1} = K_m \frac{\rho_{g,0}\, u_{g,0}^2}{2} \quad (2)$$

Suction pressure $p_{g,1}$ of mixed gases caused by liquid jet can be determined from the balance of momentum between pre mixing section and entrance to the mixing section, that means between states 0 and 1. Precise parameters are required to determine the pressure at the beginning of condensation process, namely location 1. Transition from location 0 to location 1 can be determined from the momentum balance equation of the mixture:

$$p_{g,0} A_{g,0} + m_{g,0} u_{g,0} + p_l A_j + m_l u_l = p_{g,1} A_1 + \left(m_{g,1} + m_l\right) u_l \quad (3)$$

3. Analytical Model

In this section, liquid droplet, condensation of vapour on subcooled droplet stream, heat and mass for vapour-gas mixture, effect of droplets deposition and entrainment rate due to presence of duct walls and pressure drop in mixing chamber and diffuser have been investigated analytically.

3.1 Liquid droplet

Let us now consider the averaged mass and force balance equations for the liquid drops. Stream of drops leaving the supplying water nozzle has the mass moving with the same velocity as the stream of liquid leaving the supplying channel, so the mass of droplets is the same as the mass of liquid on the length of the throat:

$$n\, m_d = \frac{\pi\, d_d^3 \rho_l}{6} n = m_{l0} = \frac{\pi\, D_d}{4}\, l\, \rho_l \quad (4)$$

where: $n=3/2(D_0/d_d)^2 l/d_d$ total number of droplet exchanging mass and heat in throat of nozzle
$n_x = x/l \times n$ number of droplets being within distance x

3.2 Condensation of vapour on subcooled droplet stream

Mass balance on the droplet's interface gives the relation:

$$\frac{dm_d}{dt} = \rho_v w_v \pi d_d^2 \quad (5)$$

Where $\dot{m}_v = \rho_v w_v$ - mass flux of condensing vapour.
Taking advantage of the Fick's Law:

$$\rho_v w_v = -D_v \frac{d\rho_v}{dn} \quad (6)$$

we obtain:

$$\frac{dm_d}{dt} = -\rho_v D_v \frac{d\omega}{dn} \pi d_d^2 = -\rho_v D_v \frac{\omega_d - \omega_\infty}{d_d} \pi d_d^2 \quad (7)$$

3.3 Heat balance of droplet stream

In order to determine temperature of droplets stream the energy balance is used:

$$\frac{d}{dx}\left(c_{pl}\dot{m}_d T_d\right) + \frac{h_{lv}}{dx} d\dot{m} = \frac{d\dot{Q}}{dx} \quad (8)$$

That means that the change of enthalpy stream of droplets and heat realised due to condensation is gained from the stream of a mixture of vapour and non-condensable gas, defined as:

$$\frac{d\dot{Q}}{dx} = \pi d_d^2 \frac{n}{l} h_{mg}(T_m - T_d) \quad (9)$$

Relation (6) presents the amount of heat supplied through the convection to interface to droplet stream, where h_{mg} is the convective heat transfer coefficient.
Introducing (7), (8) and (9) and rearranging the droplet temperature gradient of is obtained

$$\frac{dT_d}{dx} = -\left(\frac{T_d}{\dot{m}_d} + \frac{h_{lv}}{c_{pl}\dot{m}_d}\right)\frac{d\dot{m}}{dx} + \frac{\pi d_d^2 \frac{n}{l} h_{mg}(T_m - T_d)}{c_{pl}\dot{m}_d} \quad (10)$$

3.4 Balance of mass and heat for vapour-gas mixture

Balance of mass for the mixture of vapour and gas rate is

$$\dot{m}_m(x) = \dot{m}_{m0} - \int_0^l \frac{d\dot{m}_d(x)}{dx} dx \quad (11)$$

Temperature of flowing vapour-gas mixture can be determined from the balance of heat for the mixture of vapour-gas flow as:

$$-c_{pm} d(\dot{m}_m T_m) = d\dot{Q} = \frac{h_m \pi d_d^2 n}{l}(T_m - T_d)dx \quad (12)$$

$$\frac{dT_m}{dx} = -\frac{T_m}{\dot{m}_m}\frac{d\dot{m}}{dx} - \frac{h_m \pi d_d^2 n}{l\, \dot{m}_m c_{pm}}(T_m - T_d) \quad (13)$$

4. Model Validation

The analytical pressure data was compared with predictions resulting from the experimental models described by Silva [19]. Her experimental venturi scrubber facility has a throat diameter of 125 mm and a total length of 1.27 m. The throat gas velocity was within the range between 34 and 70 m/s and the liquid flow rate was set between 0.013 and 0.075 (kg/s). For validation, liquid flow rate was considered 0.038 and gas flow rate was supposed 0.483, 0.736, 0.861 and 0.987(kg/s), respectively. As it can be seen in Fig. 3. good agreement was achieved between the experimental results data taken from the studies by Silva.

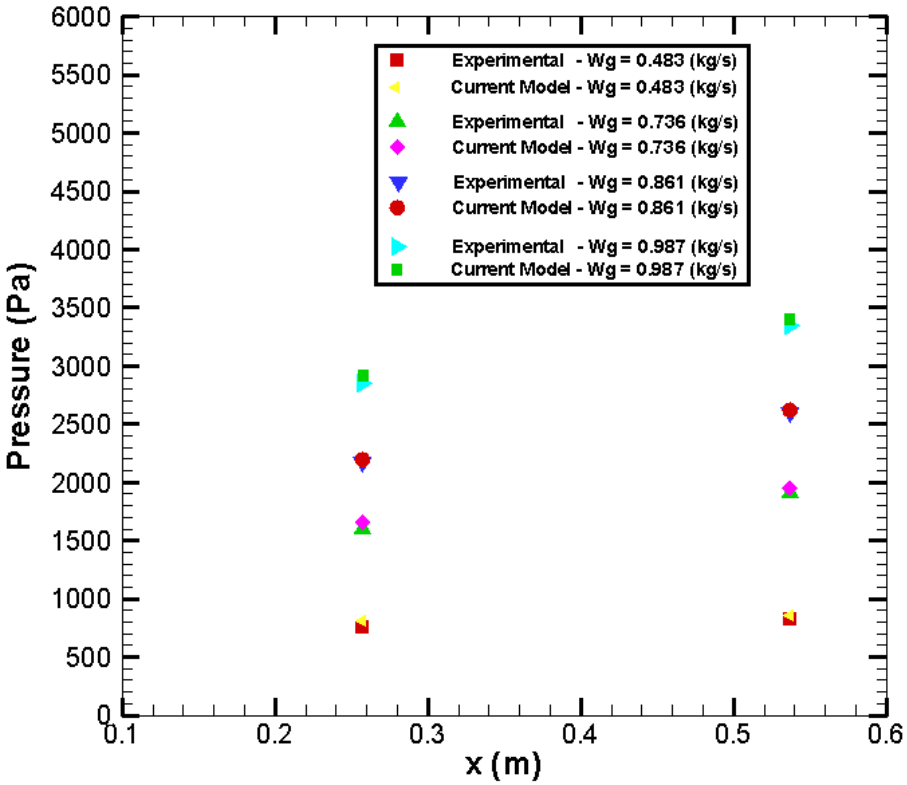

Fig. 3. Validation

5.Results and discussions

5.1 Effect of breakup of droplets

In this section, it is assumed that there will be an extra zone prior to the liquid breakup into droplets, followed by the breakup. The liquid stream breaks into droplets under the influence of waves formed on the surface of the stream due to instability. These waves cause a loss of stability and the formation of primary droplets. The size of these droplets results from the volume of the wave and the formation of droplets with a minimum surface energy. For certain outflow conditions of a liquid jet, there is an optimum wavelength whose length is greater than the jet circumference, at which the wave amplitude increases and the liquid jet bursts. Weber developed a relation for the size of primary droplets:

$$\frac{D}{Dj} = 1.436\left(1 + 3\frac{We^{0.5}}{Re}\right)^{1/6} \tag{14}$$

where :$We = \frac{\rho_l u_l^2 D_j}{\sigma_l}$ – Weber number, R$e = \frac{\rho_l u_l D_j}{\mu_l}$ - Reynolds number

For $We > We_{cr}$ as a criterion for the beginning of liquid stream breakup it has been assumed that $We_{cr} = 14$.
Length of the zone from which primary droplets are formed from a turbulent liquid stream yields:

$$\frac{L}{Dj} = 11.5We^{0.31} \quad (15)$$

Secondary droplet breakup occurs under the influence of aerodynamic forces. Primary droplets are deformed and broken up by aerodynamic drag forces and surface tension forces. The maximum droplet size can be determined from the relationship:

$$D_{max} = \frac{\sigma We_{cr}}{\rho_g (u_l - u_g)^2} \quad (16)$$

The average droplet size can be taken as:

$$D_m = \frac{D_{max}}{2} \quad (17)$$

A more accurate value can be calculated from the droplet size distribution spectrum.
After using aforementioned equations, the maximum droplet diameter is 3 mm, so in practice a value of 1.5 mm can be assumed as a best estimate. If we consider $D_0 = 7\ mm$, the number of droplet will be 4356. So, the distributions of temperature of droplet and mixture of steam for different initial velocity of droplet are depicted in Figs. 4 and 5, respectively. Increasing the value of initial velocity of droplet from 25 to 150 (m/s) causes decline the temperature of droplet in the length of throat (x=0.2 m), so that the maximum value of the temperature of droplet take place at x=0.2 m and Ud_0 = 25. On the other hand, the temperature of mixture of steam has been faced with a falling trend along the throat, so that the maximum value for that happens at x=0 m and Ud_0 = 25.
In addition, having studied the data from Figs 6 and 7, it can be considered that increasing the value of Um0 not only results in increasing the temperature of droplet, but also leads to rise the temperature of mixture of steam at the length of throat. Moreover, the lowest value for temperature of droplet and mixture of steam is when the drop is moving in stagnant environment $(u_m(x) = 0)$.

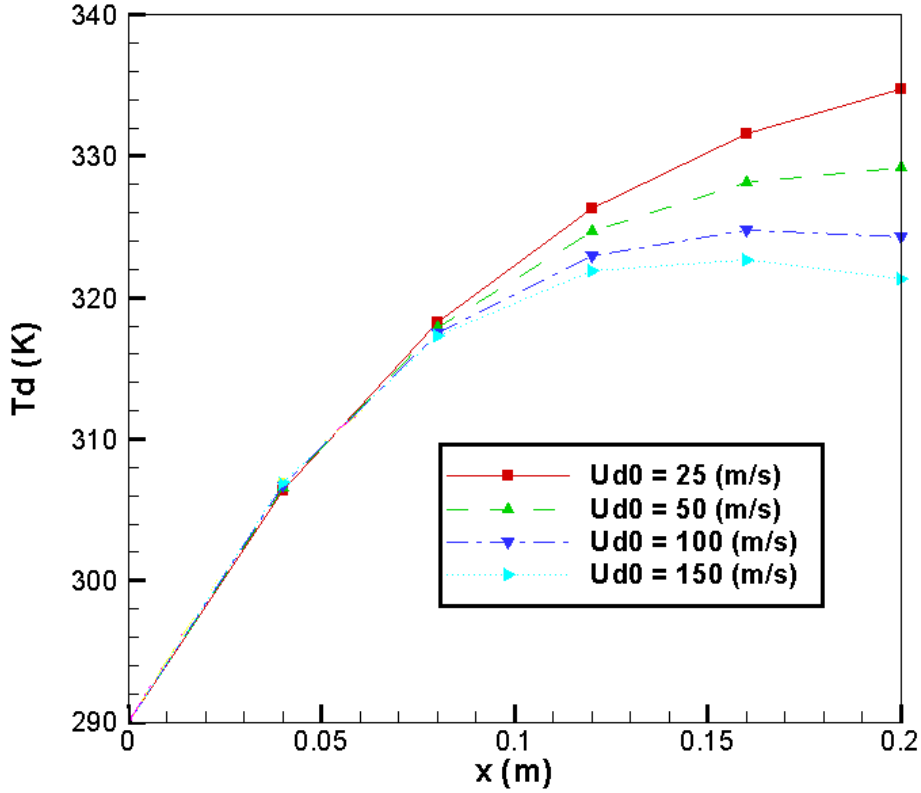

Fig. 4. Distribution of temperature of droplet for different initial velocity of droplet at Um_0=20 m/s and diameter of droplet 1.5 mm

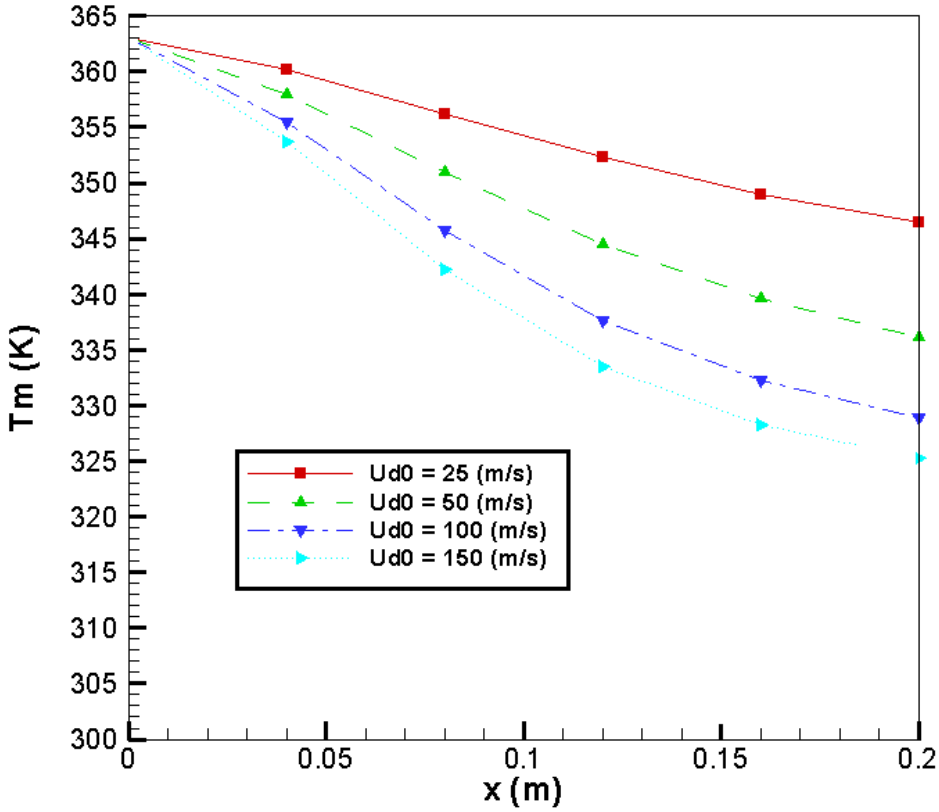

Fig. 5. Distribution of temperature of mixture of steam for different initial velocity of droplet at Um_0=20 m/s and diameter of droplet 1.5 mm

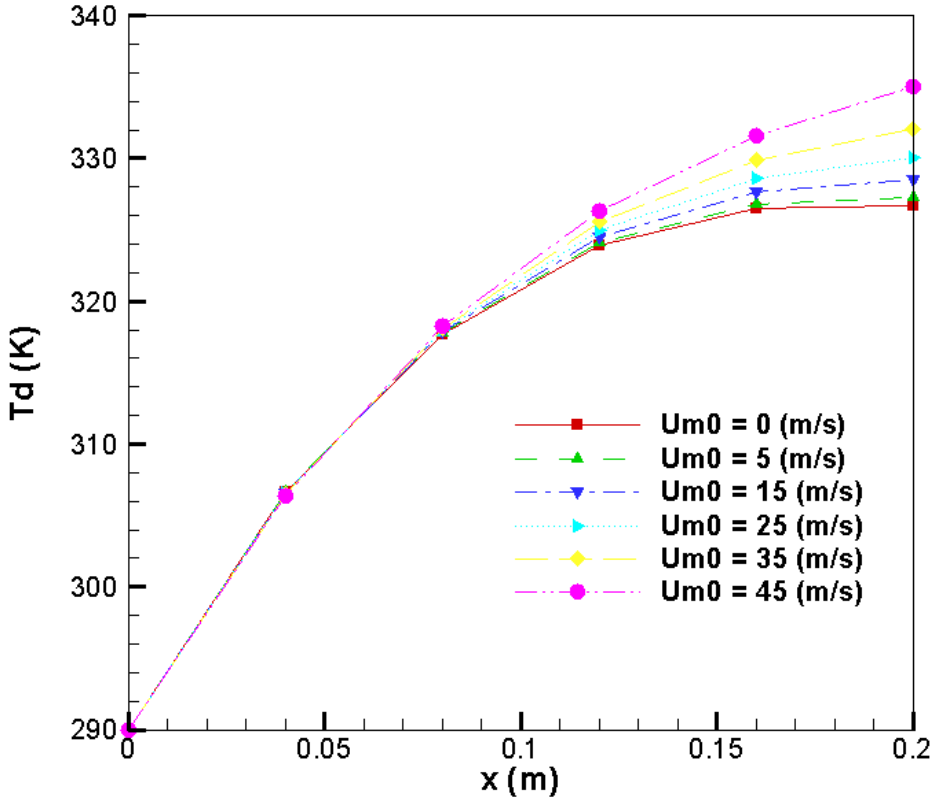

Fig. 6. Distribution of temperature of droplet for different initial velocity of mixture at Ud_0=50 m/s and diameter of droplet 1.5 mm

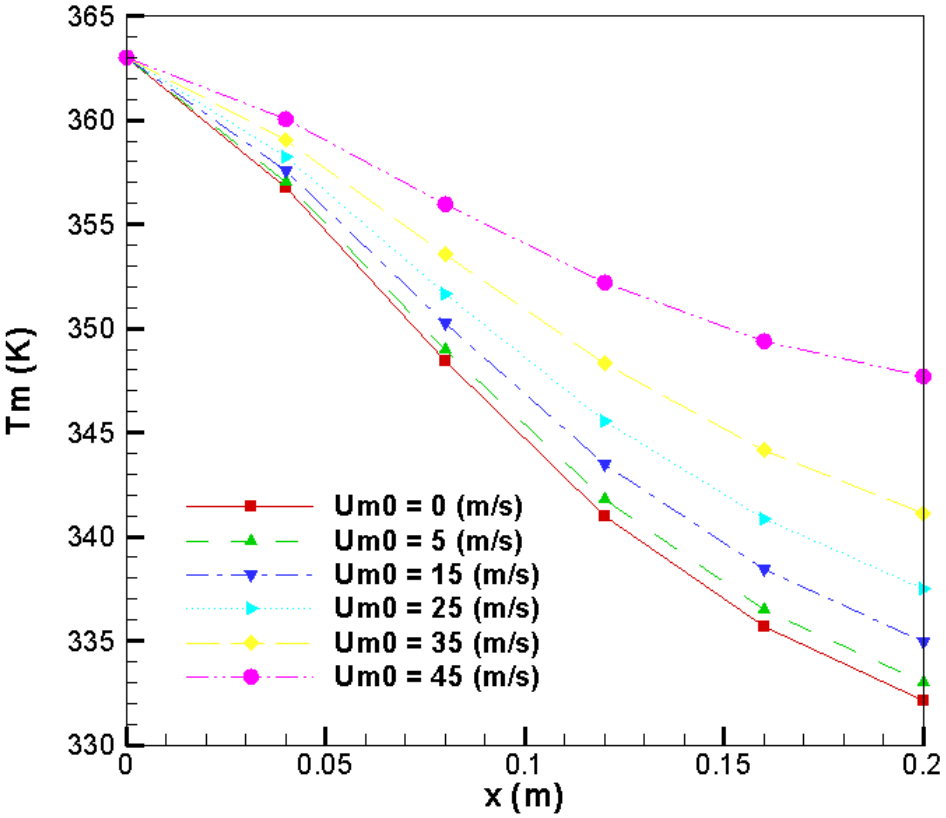

Fig. 7. Distribution of temperature of mixture of steam for different initial velocity of mixture at Ud_0=50 m/s and diameter of droplet 1.5 mm

5.2 Effect of throat diameter

Figures 8 and 9 depict distribution of temperature of droplets and mixture of steam for different values of diameter of throat, respectively. Ud_0=50 m/s, Um_0=20 m/s and diameter of droplet 1.5 mm have been considered. Results show that although the temperature of droplets is faced with a rising trend for 3, 5, and 7 mm of diameter of throat, it reaches a maximum value for 9 mm of diameter of throat at x=0.12 m, and, then decreases gradually. Temperature of mixture of steam declines for mentioned diameter of throat along the length of throat.

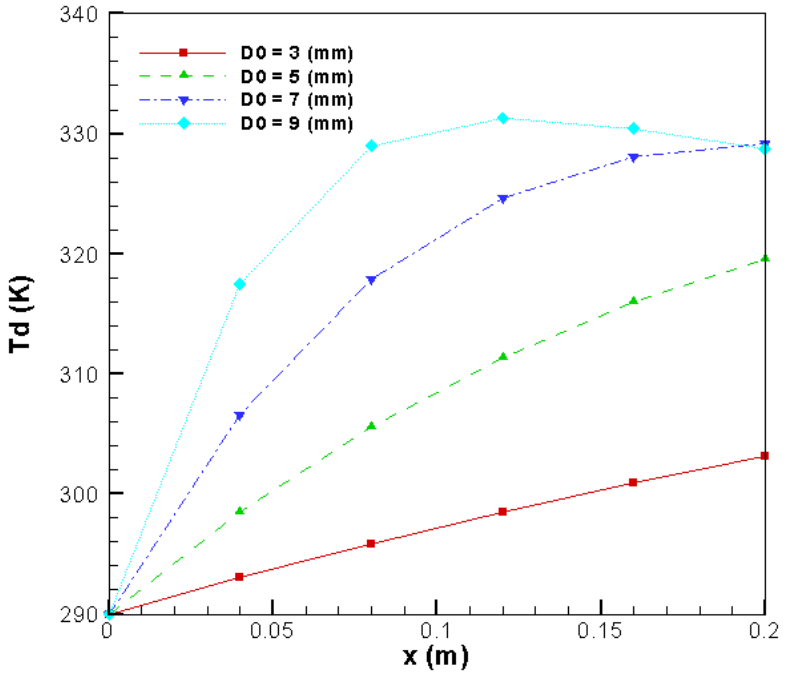

Fig. 8. Distribution of temperature of droplet for different D0 at Ud_0=50 m/s and Um_0=20 m/s and diameter of droplet 1.5 mm

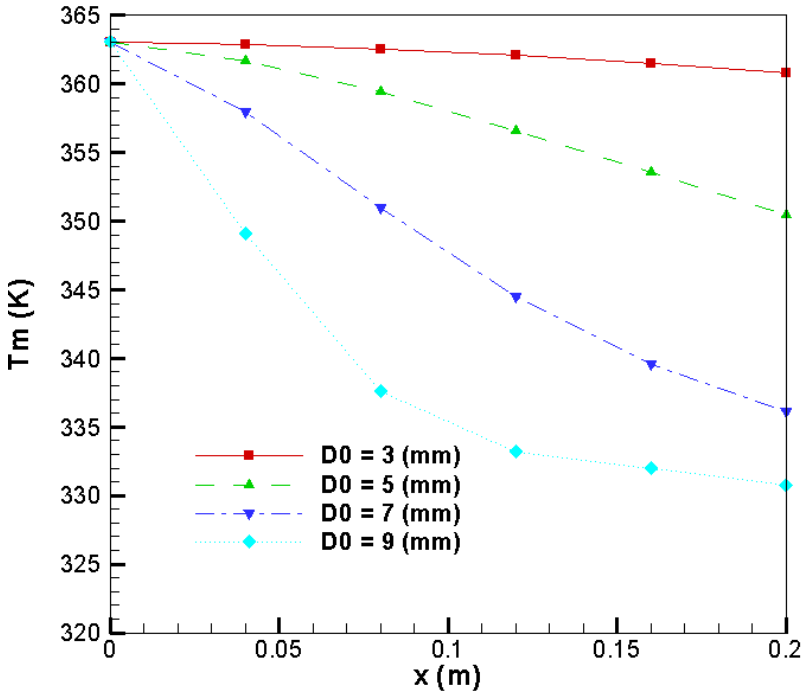

Fig. 9. Distribution of temperature of mixture of steam for different D0 at Ud_0=50 m/s and Um_0=20 m/s and diameter of droplet 1.5 mm

6. CONCLUSIONS

An analytical study on the steam–water direct contact condensation was conducted to investigate the thermal characteristics of these phenomena. Through the thermal analysis, the following results were found in accordance to the following:

- Increasing the value of initial velocity of mixture of steam (Um0) not only results in increasing the temperature of droplet, but also leads to rise the temperature of mixture of steam at the length of throat.
- The lowest value for temperature of droplet and mixture of steam is when the drop is moving in stagnant environment $(u_m(x) = 0)$.
- Given the finding that the diameter of droplet can be correlated with considering extra zone prior to the liquid breakup into droplets, followed by the breakup and 1.5 (mm) of diameter of droplet is the best estimate.
- Although the temperature of droplets is faced with a rising trend for 3, 5, and 7 mm of diameter of throat, it reaches a maximum value for 9 mm of diameter of throat at x=0.12 m, and, then decreases gradually.
- Temperature of mixture of steam declines for mentioned diameter of throat along the length of throat.

Acknowledgments : The research leading to these results has received funding from the Norway Grants 2014-2021 via the National Centre for Research and Development within the frame of the project : "Negative CO_2 emission gas power plant" - NOR/POLNORCCS/NEGATIVE-CO2-PP/0009/2019-00 which is co-financed by programme "Applied research" under the Norwegian Financial Mechanisms 2014-2021 POLNOR CCS 2019 - Development of CO2 capture solutions integrated in power and industry processes.

NOMENCLATURE

a - thermal diffusivity, m^2/s,
c_p - specific heat, J/(kg K)
C - constant (= x-d^4),
g - gravitational acceleration, m/s^2
h_m - mass transfer coefficient
$h_{m,g}$ - convection heat transfer coefficient
Ja - Jakob number (= $c_p(T_s - T_0)/h_{lv}$)
l_m - distance between the centres of neighbouring droplets
m - mass flow rate, kg/s
$\dot{m}_v$ - the mass flow rate of condensation of vapour on the droplet surface
N - total number of droplet
p - pressure, N/m^2
q - heat flux, W/m^2
R - individual gas constant
Re - Reynolds number
Sh - Sherwood number
t - time, s
T - temperature, °C
T_d - Temperature of droplet
T_m - Temperature of mixture of steam
u - velocity in the x-direction, m/s
x - coordinate along the flow measured from throat outlet
x_0 - thermal entry (development length, m)
z - ratio of droplet velocity to mixture velocity

Greek Symbols

α - local heat transfer coefficient, $W/(m^2 K)$
δ - liquid film thickness, m
μ - dynamic viscosity, kg/(m s)
ν - kinematic viscosity, m^2/s
ρ - density, kg/m^3
τ - shear stress, N/m^2
κ - the ratio of specific heat at constant pressure to specific heat at constant volume

Subscripts

c - condensation
l - liquid,
0 - initial parameter (at the slit outlet)
v - vapour
t - turbulent
x - axial component
w - wall

Superscript

+ - dimensionless value

References:

1. Kim, Y.-S., J.-W. Park, and C.-H. Song, 2004. *Investigation of the stem-water direct contact condensation heat transfer coefficients using interfacial transport models.* International Communications in Heat and Mass Transfer. **31**(3): p. 397-408.
2. Shah, A., I.R. Chughtai, and M.H. Inayat, 2014. *Experimental and numerical investigation of the effect of mixing section length on direct-contact condensation in steam jet pump.* International Journal of Heat and Mass Transfer. **72**: p. 430-439.
3. Xu, Q. and L. Guo, 2016. *Direct contact condensation of steam jet in crossflow of water in a vertical pipe. Experimental investigation on condensation regime diagram and jet penetration length.* International Journal of Heat and Mass Transfer. **94**: p. 528-538.
4. Ziółkowski, P., et al., 2021. *Thermodynamic Analysis of Negative CO2 Emission Power Plant Using Aspen Plus, Aspen Hysys, and Ebsilon Software.* Energies. **14**(19): p. 6304.
5. Ziółkowski, P., et al., 2022. *Mathematical modelling of gasification process of sewage sludge in reactor of negative CO2 emission power plant.* Energy. **244**: p. 122601.
6. Kreith, F. and R. Boehm, 2013. *Direct-contact heat transfer*: Springer Science & Business Media.
7. Li, Y., et al., 2011. *Pressure wave propagation characteristics in a two-phase flow pipeline for liquid-propellant rocket.* Aerospace Science and Technology,. **15**(6): p. 453-464.
8. Kang, Z., et al., 2018. *Numerical investigation on flow condensation process during interphase mixing in oxygen pipeline of liquid rocket.* Asia‐Pacific Journal of Chemical Engineering,. **13**(5): p. e2235.
9. Jayachandran, K., R. Arnab, and G. Parthasarathi. 2017. *Numerical investigations on unstable direct contact condensation of cryogenic fluids*. in *IOP Conference Series: Materials Science and Engineering*. IOP Publishing.
10. KN, J., A. Roy, and P. Ghosh. 2017. *Numerical Studies on Direct Contact Condensation (DCC) of Subsonic Vapor/Gas Jets in Subcooled Flowing Liquid*. in *55th AIAA Aerospace Sciences Meeting*.
11. Jayachandran, K., A. Roy, and P. Ghosh, 2018. *Numerical investigations on direct contact condensation (DCC) of oxygen vapour in a staged combustion cycle based rocket engine*.
12. Li, S., P. Wang, and T. Lu, 2015. *CFD based approach for modeling steam–water direct contact condensation in subcooled water flow in a tee junction.* Progress in Nuclear Energy. **85**: p. 729-746.
13. Li, J., et al., 2022. *Secondary droplet size distribution upon breakup of a sub-milimeter droplet in high speed cross flow.* International Journal of Multiphase Flow. **148**: p. 103943.
14. Guan, B., et al., 2018. *Numerical study on liquid droplet internal flow under shock impact.* AIAA journal,. **56**(9): p. 3382-3387.
15. Meng, J.C. and T. Colonius, 2018. *Numerical simulation of the aerobreakup of a water droplet.* Journal of Fluid Mechanics. **835**: p. 1108-1135.
16. Stefanitsis, D., et al., 2021. *Numerical Investigation of the Aerodynamic Droplet Breakup at Mach Numbers Greater Than 1*. Journal of Energy Engineering. **147**(1): p. 04020077.
17. Shen, S., et al., 2019. *The effect of the weber number on the droplet deformation and breakup process before a standing wall.* Atomization and Sprays. **29**(11).
18. Shen, S., et al., 2019. *The viscous effect on the transient droplet deformation process under the action of shock wave.* Atomization and Sprays. **29**(2).
19. Silva, A., 2008. *Numerical and experimental study of venturi scrubbers*.